Memetic Search for Green Vehicle Routing Problem with Private Capacitated Refueling Stations

Rui Xu, Xing Fan, Shengcai Liu, Wenjie Chen, and Ke Tang

arXiv:2504.04527v1 [cs.NE] 6 Apr 2025

Abstract—The green vehicle routing problem with private capacitated alternative fuel stations (GVRP-PCAFS) extends the traditional green vehicle routing problem by considering refueling stations limited capacity, where a limited number of vehicles can refuel simultaneously with additional vehicles must wait. This feature presents new challenges for route planning, as waiting times at stations must be managed while keeping route durations within limits and reducing total travel distance. This article presents METS, a novel memetic algorithm (MA) with separate constraint-based tour segmentation (SCTS) and efficient local search (ELS) for solving GVRP-PCAFS. METS combines global and local search effectively through three novelties. For global search, the SCTS strategy splits giant tours to generate diverse solutions, and the search process is guided by a comprehensive fitness evaluation function to dynamically control feasibility and diversity to produce solutions that are both diverse and near-feasible. For local search, ELS incorporates tailored move operators with constant-time move evaluation mechanisms, enabling efficient exploration of large solution neighborhoods. Experimental results demonstrate that METS discovers 31 new best-known solutions out of 40 instances in existing benchmark sets, achieving substantial improvements over current state-of-the-art methods. Additionally, a new large-scale benchmark set based on real-world logistics data is introduced to facilitate future research.

Index Terms—Green vehicle routing problem, memetic algorithm, private capacitated alternative refueling stations, real-world applications

I. INTRODUCTION

AS environmental concerns grow and sustainable logistics becomes increasingly critical, the green vehicle routing problem (GVRP) [1] has emerged as an essential challenge in modern transportation systems [2]–[4]. Specifically, GVRP focuses on planning routes for alternative fuel vehicles (AFVs), e.g., electric vehicles, to serve customers while considering AFVs' limited driving range and need for refueling. A good route plan should minimize travel distance while ensuring timely refueling. In the classic GVRP model [1], it is assumed that the alternative fuel stations (AFSs) have unlimited service spots (capacity), meaning vehicles can refuel immediately upon arrival without waiting times.

R. Xu and X. Fan are with the School of Business, Hohai University, Nanjing 211100, China, and with the Guangdong Provincial Key Laboratory of Brain-inspired Intelligent Computation, Southern University of Science and Technology, Shenzhen 518055, China (e-mail: rxu@hhu.edu.cn; fanxingbozhou@outlook.com).

S. Liu and K. Tang are with the Guangdong Provincial Key Laboratory of Brain-inspired Intelligent Computation, Department of Computer Science and Engineering, Southern University of Science and Technology, Shenzhen 518055, China (e-mail: liusc3@sustech.edu.cn; tangk3@sustech.edu.cn).

W. Chen is with the School of Information Management, Central China Normal University, Wuhan, China.(e-mail: chenwj6@ccnu.edu.cn).

(a) All AFVs depart from the depot. **(b) AFV 2 refuels while AFV 3 waits.** **(c) AFV 3 exceeds the time duration limit.**

Depot / Customer / AFV / Refueling / Waiting to Refuel / Current Time Indicator / Available AFS / Occupied AFS

(d) AFV 2 refuels, AFV 3 avoids waiting. **(e) All AFVs have returned to the depot.**
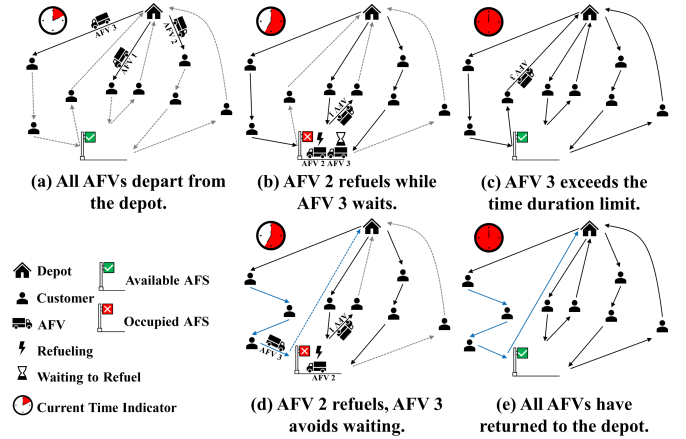
Fig. 1. Illustrations of vehicle waiting caused by the limited capacity at AFS in GVRP-PCAFS with three AFVs, eight customers, and one AFS that can serve one vehicle at the same time. **(a)** Three AFVs depart from the depot. **(b)** During service, AFV 2 is refueling while AFV 3 arrives at the same station and must wait. **(c)** AFS 3 exceeds the route duration limit due to waiting for refueling. **(d)** After adjusting the route plan (the blue line), AFS 3 serves customers first and then refuels at the AFS, thus avoiding crowding at the AFS. **(e)** All AFVs complete their routes within the route duration limit.

This assumption, however, does not always hold in real-world scenarios where AFSs often have a limited number of charging pumps or refueling spots [5]. Among various scenarios involving AFSs with limited capacity, Bruglieri *et al.* [6] studied the typical case where logistics companies operate their own private AFSs and introduced the GVRP with private capacitated alternative fuel stations (GVRP-PCAFS). In GVRP-PCAFS, each AFS can only serve a limited number of vehicles simultaneously and any additional vehicle must wait until a refueling spot becomes available. Compared to the classic GVRP, which is already NP-hard, GVRP-PCAFS is even more challenging to solve due to the added complexity of managing waiting times and ensuring route durations do not exceed a given time limit. Examples of route plans for GVRP-PCAFS are demonstrated in Figure 1, where the AFS can serve only one vehicle at the same time, and waiting times at the AFS eventually cause route duration to exceed the limit (Figure 1(b)-1(c)). Through adjusting the visiting sequence of customers and AFS in the route plan, such waiting times and route duration violations are avoided (Figure 1(d)-1(e)).

Existing approaches for solving GVRP-PCAFS can be classified into exact methods and heuristic methods. However, neither approach has shown fully satisfactory performance. Exact methods, such as cutting plane techniques [6], [7],

guarantee optimality but are restricted to small-scale instances, due to their exponential time complexity. Heuristic methods, like the GRASP algorithm [8], aim to address larger instances. However, our experiments find that for medium-scale instances with 50 and 100 customers, there is still considerable room for improvement in solution quality obtained by existing heuristic methods. Furthermore, research on large-scale GVRP-PCAFS instances remains limited. The largest problem instance in the publicly available benchmark set [8] contains only 100 customers. In contrast, with the rapid growth of urban areas, a real-world GVRP-PCAFS instance might involve many more customers. For example, based on our collected data from a logistics company in Beijing, a major city in China, real-world applications regularly handle instances with up to 1000 customers (see Section IV for details). In summary, these observations indicate notable research gaps in both developing high-performing algorithms for solving GVRP-PCAFS and establishing benchmark sets that can better reflect real-world problem sizes.

This work aims to address the above limitations. Specifically, a novel **me**metic algorithm with separate constraint-based **t**our segmentation and efficient local **s**earch, dubbed METS, is proposed to solve GVRP-PCAFS. Memetic algorithms (MAs), which combine global search strategies (e.g., crossover) with local search heuristics, are an important class of Evolutionary Algorithms (EAs) and have been the state-of-the-art methods on many variants of vehicle routing problems (VRPs) [9]–[11]. However, although MA provides a generic framework, developing an effective instantiation of MA for GVRP-PCAFS is non-trivial. Specifically, two main challenges need to be addressed. First, the global search of the algorithm needs to effectively promote population diversity. A common strategy is to consider both feasible and infeasible solutions during the search process. However, it is challenging to simultaneously promote diversity and appropriately control the degree of constraint violations in GVRP-PCAFS, since infeasible solutions with severe constraint violations, despite being diverse, cannot provide valuable solution information, e.g., patterns of customer sequences. This is termed as the diversity-feasibility control challenge. Second, an efficient local search procedure is essential for a high-performing MA. This procedure should incorporate move operators tailored to GVRP-PCAFS to explore neighborhood solution space, with high computational efficiency.

METS integrates several novel features to comprehensively address the above two aspects. First, for the global search, the giant-tour solution representation, which encodes a solution as a single permutation of all customers, is adopted for population initialization and crossover in METS. To generate diverse solutions based on the giant tours, a new separate constraint-based tour split (SCTS) strategy is proposed that splits a giant tour into routes using a randomly selected single constraint, thereby producing distinct solutions. To tackle the diversity-feasibility control challenge, a comprehensive fitness evaluation function is introduced in METS that simultaneously takes into account solution costs, constraint violation degrees, and diversity contribution. Through adaptive adjustment of weighting parameters for these terms, METS effectively con-

trols population diversity and feasibility during the search process. Second, for the local search procedure, a conditional AFS-insertion rule (CAI) is introduced to automatically determine whether to insert an AFS based on the route's current state. Four new move operators are derived from CAI rule, which effectively combines AFS insertion and customer adjustments into a single move. Additionally, a constant-time move evaluation mechanism is proposed for these operators, significantly reducing computational overhead of the local search procedure.

The main contributions of this work are summarized below.

- A novel memetic algorithm called METS is proposed for solving GVRP-PCAFS. The algorithm has three novelties: a SCTS strategy to promote solution diversity, a comprehensive fitness evaluation function for effectively controlling diversity and feasibility among population, and a highly efficient local search procedure with specialized move operators tailored to GVRP-PCAFS.
- Experiments show that METS discovers 31 **new** best-known solutions out of 40 instances in the existing benchmark set, demonstrating improvements by large margin over current state-of-the-art methods.
- A new large-scale benchmark set for GVRP-PCAFS is established based on real-world logistics data collected from Beijing, featuring problem instances with up to 1,000 customers. Both the benchmark instances and the source code of METS will be made publicly available to support future research.

The rest of the article is organized as follows. Section II presents the problem description and literature review. Section III first introduces the novel features of METS, followed by the description of its framework. Section IV compares METS with existing methods on existing benchmark set and the new benchmark set introduced in this work. Finally, conclusions and future directions are provided in Section V.

II. PROBLEM DESCRIPTION AND RELATED WORK

A. Notations and Problem Formulation

Formally, the GVRP-PCAFS [6] is defined on a complete directed graph $G = (V, E)$, where $V = \{0\} \cup V_c \cup F = \{0, 1, 2, \ldots, n, n+1, \ldots, n+s\}$ is the node set and 0 represents the depot. $V_c = \{1, 2, \ldots, n\}$ is a set of n customers and $F = \{n + 1, n + 2, \ldots, n + s\}$ is a set of s AFSs. The edge set $E = \{(i, j) \mid i, j \in V, i \neq j\}$ is defined between each pair of vertices. Each customer $i \in V_c$ has a service time $\tau(i)$ and each edge $(i, j) \in E$ is associated with a travel time $t_{i,j}$ and a travel distance $d_{i,j}$.

The problem involves a homogeneous fleet of M AFVs initially located at the depot. The AFVs depart from the depot with full energy level E_f, serve each customer exactly once, and return to the depot. Each AFV must adhere to a route duration limit T_{max} that includes travel time, waiting time, and service time. This duration constraint ensures that drivers are not overworked (complying with transportation regulations) and that customers are served within a reasonable period. The AFVs consume energy at a rate cr while traveling, i.e., the maximum driving range D_{max} is determined by the full

energy level E_f and the energy consumption rate, calculated as $D_{max} = \frac{E_f}{cr}$. An AFV must visit an AFS to refuel to the full energy level E_f before depleting its energy, with a constant refueling time $\tau(s)$. Following Bruglieri *et al.* [6], this work focuses on small package delivery scenarios where vehicles are assumed to have unlimited capacity. To avoid confusion, the term "capacity(η_s)" in this article refers specifically to AFSs, indicating the maximum number of vehicles that can be serviced simultaneously at each AFS.

A solution φ to GVRP-PCAFS is represented by a set of vehicle routes, $\varphi = \{r_1, r_2, ..., r_h\}$, where h is the number of AFVs used. Each route r_i consists of a sequence of nodes that the AFV visits, i.e., $r_i = (x_{i,1}, x_{i,2}, ..., x_{i,k_i})$, where $x_{i,j}$ is the j-th node visited in r_i and k_i is the length of r_i. For brevity, below we temporarily omit the subscript i in r_i, i.e., $r = (x_1, x_2, ..., x_k)$. The total travel distance of r, denoted as $TD(r)$, is:

$$TD(r) = \sum_{j=1}^{k-1} d_{x_j, x_{j+1}}. \tag{1}$$

An AFV departs from the depot with full energy level E_f. The energy level of the AFV on arrival at and departure from x_j, denoted as l_{x_j} and L_{x_j}, respectively, can be computed recursively as follows:

$$l_{x_j} = L_{x_{j-1}} - cr \cdot d_{x_{j-1}, x_j}, \quad j > 1,$$
$$L_{x_j} = \begin{cases} E_f, & j = 1 \vee x_j \in F, \\ l_{x_j}, & j > 1 \wedge x_j \notin F. \end{cases} \tag{2}$$

The arrival and departure time at x_j, denoted as arr_{x_j} and dep_{x_j}, respectively, can be computed recursively as follows:

$$arr_{x_j} = dep_{x_{j-1}} + t_{x_{j-1}, x_j}, \quad j > 1,$$
$$dep_{x_j} = \begin{cases} 0, & j = 1, \\ arr_{x_j} + \tau(x_j), & j > 1 \wedge x_j \notin F, \\ arr_{x_j} + \tau(s) + WT(x_j), & j > 1 \wedge x_j \in F. \end{cases} \tag{3}$$

$\tau(x_j)$ and $\tau(s)$ are the service time at the customer and refueling time at the AFS, respectively. The waiting time $WT(x_j)$ at the AFS is determined by the scheduling procedure introduced in Bruglieri *et al.* [8]. This procedure schedules the refueling sequence for all vehicles at the AFS while ensuring that at any time, the number of simultaneously refueling vehicles does not exceed the AFS's capacity η_s. If the number of vehicles requiring refueling exceeds this capacity, vehicles scheduled for later refueling slots must wait. For details of the procedure, please refer to [8]. Hence, the duration of route r, denoted as $TM(r)$, is:

$$TM(r) = arr_{x_k} - dep_{x_1} = arr_{x_k}. \tag{4}$$

which is the arrival time at the last visited node x_k.

Finally, the objective is to find a solution φ that minimizes the total travel distance $TD(\varphi)$, as presented in Eq. (5):

$$\min_{\varphi} TD(\varphi) = \sum_{i=1}^{h} TD(r_i), \tag{5a}$$

$$\text{s.t. } x_{i,1} = x_{i,k_i} = 0, \quad 1 \le i \le h, \tag{5b}$$

$$\sum_{i=1}^{h} \sum_{j=2}^{k_i-1} \mathbb{I}[x_{i,j} = z] = 1, \quad 1 \le z \le n, \tag{5c}$$

$$0 < h \le M, \tag{5d}$$

$$0 \le TM(r_i) \le T_{max}, 1 \le i \le h, \tag{5e}$$

$$0 \le l_{x_{i,j}} \le L_{x_{i,j}} \le E_f, 1 \le i \le h, 1 \le j \le k_i. \tag{5f}$$

The constraints are explained as follows: 5b) Each route must start and end at the depot; 5c) Each customer must be served exactly once (with $\mathbb{I}$ as the indicator function); 5d) The number of used vehicles cannot exceed the available vehicles; 5e) Each route must comply with the duration limit; 5f) Each AFV must always maintain a non-negative energy level.

B. Related Work

Given that AFSs often have a limited number of refueling spots in practice, Bruglieri *et al.* [6] introduced GVRP-CAFS as the first GVRP model to consider the capacity of AFSs. They developed both arc-based and path-based mixed integer linear programming (MILP) models, with corresponding cutting plane methods to solve problem instances with up to 15 customers optimally within acceptable computational time. Their later work [7] further improved these models to address the path cloning issues caused by multiple pumps at AFSs. To handle larger problem instances, the same authors proposed a greedy randomized adaptive search algorithm (GRASP) [8] that combines biased random construction and local search. They also introduced a scheduling procedure with theoretical guarantees for coordinating multiple vehicles requiring refueling at the same AFS, while considering the limited capacity of the AFSs. Their experimental results showed that GRASP could find high-quality solutions on benchmark instances with up to 100 customers, compared to previous exact methods [7]. This effective heuristic approach serves as an important reference algorithm for our study.

Besides the above studies, other researchers [12]–[14] have also investigated GVRPs with limited AFS capacity. In these studies, vehicle waiting times at AFSs are modeled by queuing processes that operate independently of vehicle routes. This means route planning cannot influence the queuing dynamics at AFSs. In contrast, GVRP-PCAFS requires route plans to be made explicitly to reduce congestion at AFSs, thereby avoiding long waiting times. From a practical point of view, these two types of approaches are suitable for different scenarios. Specifically, the queuing-based approaches [12]–[14] are well-suited for modeling public refueling stations, where individual companies have limited control over the overall queuing process. GVRP-PCAFS [6]–[8] is well-suited to model scenarios involving private refueling stations, where the logistics company can coordinate all vehicle routes to manage congestion at the stations.
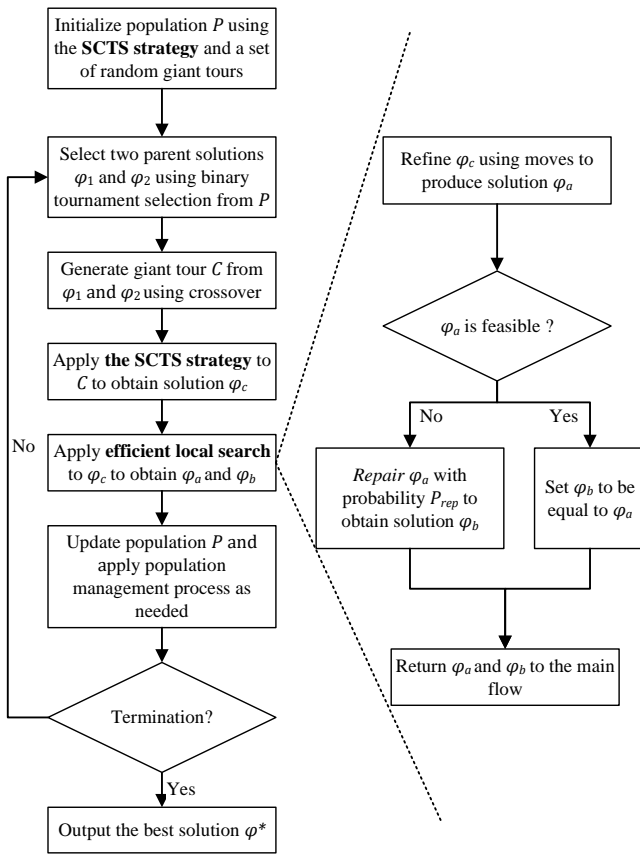
Fig. 2. The flowchart of METS.

As an important class of EAs, MAs have achieved success on a wide range of complex optimization problems [15]–[19]. Specifically, MAs have been the state-of-the-art methods for various VRPs, including the traveling salesman problem (TSP) [11], [20], capacitated vehicle routing problem (CVRP) [21], [22], vehicle routing problem with time windows (VRPTW) [10], [23], vehicle routing with simultaneous pickup-delivery and time windows (VRPSPDTW) [24], [25], electric vehicle routing problem (EVRP) [4], [26], and routing problems with intermediate facilities [27]. Compared to these problems, GVRP-PCAFS is primarily distinguished by its requirement to explicitly consider potential waiting times at AFSs to avoid route duration violations. Given this, instantiating MAs to GVRP-PCAFS requires carefully incorporating problem-specific knowledge into the algorithm design, including global search and local search heuristics. In the next section, the proposed METS algorithm is presented.

III. MEMETIC SEARCH FOR GVRP-PCAFS

This section first presents the three novel components of METS: the separate constraint-based tour split (SCTS) strategy, the comprehensive fitness evaluation function, and the efficient local search (ELS). Then, the overall framework of METS is presented. Figure 2 illustrates the flowchart of METS.

A. Splitting Giant Tours by the SCTS Strategy

Like many VRP studies [28]–[33], this paper applies the giant-tour representation due to its natural compatibility with sequence-based crossover operators such as the order crossover (OX) [34]. For the giant-tour representation, a giant tour first encodes a solution as a permutation of all customers and then is split into routes to form a complete solution. Existing splitting methods for giant tours in VRPs always consider multiple constraints simultaneously. While this helps generate feasible solutions, it often limits diversity and requires managing constraint interactions.

A novel separate constraint-based tour segmentation (SCTS) strategy is proposed, which uses a single constraint to split the giant tour in each operation. By decoupling multiple constraints, SCTS generates structurally diverse solutions and promotes population diversity during global search. In SCTS, two splitting procedures, $splitT_{max}$ and $splitD_{max}$, are developed. Specifically, the $splitT_{max}$ procedure splits the giant tour based on the route duration limit constraint, and $splitD_{max}$ divides the giant tour considering the maximum driving range constraint. Algorithm 1 presents the details of the SCTS strategy.

In Algorithm 1, SCTS takes the giant tour C containing all customers, the route duration limit T_{max}, and the maximum driving range D_{max} as input, and returns a set of routes as the output φ_c. A random number ρ is first generated (line 1). Based on the value of ρ, one of the splitting procedures is selected to obtain the solution φ_c, and each of them is chosen with probability 50% (lines 2-6). Both of the splitting procedures return a solution φ_c (line 6).

For the procedure $splitT_{max}(C, T_{max})$, it starts by initializing an empty set of routes φ_c and a counter i (line 8). Then, as long as the giant tour C is not empty (line 9), a new route r_i is created as $(depot, depot)$, indicating that the route starts and ends at the depot (line 10). Next, the loop iterates to insert customers from the giant tour on condition that the giant tour C is not empty. Specifically, in each iteration, the first customer γ from C is selected and inserted into the route r_i before the last depot (line 12). If $TM(r_i)$, the duration of route r_i, is less than the route duration limit T_{max} (line 13), γ is removed from C (line 14). Otherwise, γ is deleted from r_i, and the inner loop is broken (line 15). After that, the current route r_i is added to φ_c (line 17). Once all customers from C have been inserted, the procedure returns the solution φ_c (line 18).

For the procedure $splitD_{max}(C, D_{max})$, it also starts by initializing an empty set of routes φ_c and a counter i (line 20). While the giant tour C is not empty (line 21), a new route r_i is created. The $minAFS$ is determined as the AFS nearest to the depot (line 22). Then, r_i is initialized as $(depot, minAFS, depot)$, indicating that the route starts at the depot, visits the $minAFS$, and ends at the depot (line 23). Then, the loop iterates to select the customers in C. Each iteration selects the first customer γ from C and adds it to the route r_i before the $minAFS$ (line 25). For clarity, $(depot, ..., minAFS)$ and $(minAFS, ..., depot)$ represent two segments of r_i from the depot to the $minAFS$ and from

Algorithm 1: Separate Constraint-based Tour Split (SCTS)

Input: The giant tour C containing all customers, route duration limit T_{max}, maximum driving range D_{max}
Output: A solution φ_c containing a set of routes

1   Generate a random number $\rho \in (0,1)$;
2   **if** $\rho < 0.5$ **then**
3     $\varphi_c \leftarrow splitT_{max}(C, T_{max})$
4   **else**
5     $\varphi_c \leftarrow splitD_{max}(C, D_{max})$
6   **return** Solution φ_c;
7   **Procedure** $splitT_{max}$ (C, T_{max}) **:**
8     $\varphi_c \leftarrow \emptyset$, $i \leftarrow 0$;
9   **while** $C \neq \emptyset$ **do**
10      $i \leftarrow i+1$, $r_i \leftarrow$ (depot, depot);
11   **while** $C \neq \emptyset$ **do**
12   Insert first customer γ from C before the last depot in r_i;
13   **if** $TM(r_i) < T_{max}$ **then**
14   Remove γ from C
15   **else**
16   Remove γ from r_i, **break**;
17      $\varphi_c \leftarrow \varphi_c \cup r_i$;
18   **return** Solution φ_c;
19   **Procedure** $splitD_{max}$ (C, D_{max}) **:**
20     $\varphi_c \leftarrow \emptyset$, $i \leftarrow 0$;
21   **while** $C \neq \emptyset$ **do**
22      $minAFS \leftarrow$ the AFS nearest to the depot ;
23      $i \leftarrow i+1$, $r_i \leftarrow$ (depot, $minAFS$, depot)
24   **while** $C \neq \emptyset$ **do**
25   Insert first customer γ from C before $minAFS$ in r_i;
26   **if** $TD((depot, ..., minAFS)) < D_{max}$ **then**
27   Remove γ from C
28   **else**
29   Move γ after $minAFS$ in r_i;
30   **if** $TD((minAFS, ..., depot)) < D_{max}$ **then**
31   Remove γ from C
32   **else**
33   Remove γ from r_i, **break**;
34      $\varphi_c \leftarrow \varphi_c \cup r_i$;
35   **return** Solution φ_c;

Node	0	1	2	3	4	5	6	7	8	9	10	11
$d_{i-1,i}$	—	7	3	5	3	4	4	7	3	3	4	4
$d_{0,i}$	—	7	7	13	18	17	16	20	18	13	6	11
$d_{11,i}$	11	5	10	10	12	8	4	7	7	5	4	—

$D_{max} = 25$

(a) Initial giant tour   (b) First path-building loop

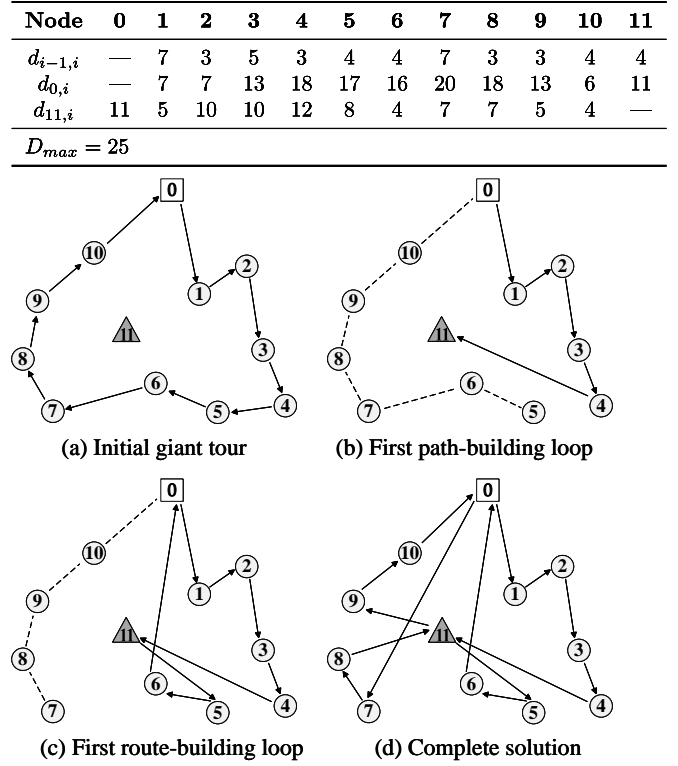(c) First route-building loop   (d) Complete solution

Fig. 3. Illustrative example of Algorithm 1 with two routes and ten customers. Node 0 represents the depot, nodes 1–10 are customer locations, and 11 denotes an AFS. The distance data table includes $d_{i-1,i}$, $d_{0,i}$, and $d_{-1,i}$, representing the distances from each node i to the previous node, depot, and AFS, respectively. D_{max} is set to 25. Figure 3(a)-1(d).

the $minAFS$ back to the depot, respectively. The ellipses indicate the omitted customers. If $TD((depot, ..., minAFS))$, the travel distance of the path $(depot, ..., minAFS)$, is less than the maximum driving range D_{max} (line 26), γ is removed from C (line 27). If D_{max} is exceeded, γ is moved after the AFS in r_i, that is, in the second route path (line 29). Next, if $TD((minAFS, ..., depot))$ is less than D_{max} (line 30), γ is removed from C (line 31). Otherwise, γ is removed from r_i, and the inner loop stops (line 33). The current route r_i is added to φ_c (line 34). Once all customers from C have been inserted, the procedure returns the solution offspring φ_c (line 35).

Figure 3 provides an example with twelve nodes (ten customers, one depot, and one AFS). Figure 3(a) shows the initial giant tour with all customers. In Figure 3(b), the first path-building loop is formed by inserting customers within the D_{max} constraint. Figure 3(c) shows the completion of the route-building loop by connecting the two paths. Figure 3(d)

displays the final solution after segmentation, where r_2 is created for the remaining customers to satisfy the D_{max} constraint.

B. Evaluating Diversity-Feasibility by the Fitness Function

A comprehensive fitness evaluation function is designed to jointly consider solution cost, constraint violation, and diversity contribution. It enables METS to adaptively control population feasibility and diversity, effectively addressing the diversity–feasibility control challenge in global search. The solution cost is measured by the total TD as defined in Eq. (5a). The constraint violation penalties and diversity contribution are introduced as follows.

1) Evaluating Feasibility: The feasibility evaluation considers three types of penalties: overtime, over-mileage, and over-capacity. Specifically, the overtime penalty applies to routes that exceed the maximum allowed duration T_{max}. The over-mileage penalty penalizes any segment of a route-either before or after refueling-that exceeds the maximum driving range D_{max} ensuring that each AFV always maintains a non-negative energy level. The over-capacity penalty applies when the number of vehicles refueling at an alternative fueling station exceeds its capacity penalizes η_s.

The penalties for overtime and over-mileage are computed using Eq. (6). Let $P(r)$ denote the total penalty of overtime and over-mileage given a route r. The parameters ω^T and ω^D are the penalty weights for overtime and over-mileage,

respectively. $path$ represents a segment of a route, that is, the portion of the route that starts from a fully refueled state (either at the depot or an AFS) and ends at the next refueling stop (an AFS) or the depot. $TM(r)$ denotes the total duration of route r as defined in Eq. (4), and $TD(path)$ denotes the travel distance of $path$ as defined in Eq. (1).

$$P(r) = \omega^T \cdot \max\{0, TM(r) - T_{max}\} + \omega^D \cdot \sum_{path \in r} \max\{0, TD(path) - D_{max}\} \quad (6)$$

The first term, $\omega^T \cdot \max\{0, TM(r) - T_{max}\}$, represents the overtime penalty, which is incurred when $TM(r)$ exceeds T_{max}. The second term, $\omega^D \cdot \sum_{path \in r} \max\{0, TD(path) - D_{max}\}$, represents the over-mileage penalty, which applies when the travel distance of any $path$ exceeds D_{max}. The summation ensures that all violating segments contribute to the total penalty. By adjusting the penalty weights ω^T and ω^D, the influence of these violations on the optimization can be controlled.

The penalty for over-capacity penalty is computed using Eq. (7). Denote $cs(s)$ as the over-capacity penalty for AFS s. Let $\mathcal{T} = \{q_1, q_2, ..., q_{2h}\}$ record the arrival and departure times of all h vehicles at the AFS, sorted in chronological order. The arrival and departure time can be calculated using Eq. (3). The initial waiting time WT for all vehicles is assumed to be 0. For a moment $q \in \mathcal{T}$, $N(q)$ represents the number of vehicles refueling at AFS s, and $\Delta(q)$ represents the time interval between moment q and the next moment $q + 1$.

$$cs(s) = \sum_{q \in \mathcal{T}} (\max\{0, N(q) - \eta_s\} \cdot \Delta(q)) \quad (7)$$

The over-capacity penalty $cs(s)$ for AFS s is calculated by summing the weighted penalties for all moments $q \in \mathcal{T}$. For each moment q, if the number of AFVs $N(q)$ exceeds η_s, the excess $N(q) - \eta_s$ is weighted by the time interval $\Delta(q)$, and the total penalty is the sum of these weighted excesses.

The total penalty $P(\varphi)$ for a solution φ is computed using Eq. (8). Specifically, $P(\varphi)$ is obtained by summing the penalties for all routes $r \in \varphi$ and the over-capacity penalties for all AFSs $s \in S$ in the solution. The penalty for each route $P(r)$ is computed using Eq. (6), and the over-capacity penalty for each AFS is computed using Eq. (7). The parameter ω^C represents the penalty weight for over-capacity.

$$P(\varphi) = \sum_{r \in \varphi} P(r) + \omega^C \cdot \sum_{s \in S} cs(s) \quad (8)$$

2) Evaluating Diversity: The diversity contribution of individuals is evaluated by the normalized Hamming distance $\xi(\varphi, \varphi')$ as shown in Eq. (9). $preA_\varphi(i)$ and $preA_{\varphi'}(i)$ denote the arcs from the previous point to the customer i in individuals φ and φ', respectively. $suA_\varphi(i)$ and $suA_{\varphi'}(i)$ represent the arcs from the customer i to the next point in individuals φ and φ', respectively.

$$\xi(\varphi, \varphi') = \frac{1}{2n} \sum_{i=1}^{n} [$$
$$1\,(preA_\varphi(i) \neq preA_{\varphi'}(i) \cap preA_\varphi(i) \neq suA_{\varphi'}(i))$$
$$+ 1\,(suA_\varphi(i) \neq suA_{\varphi'}(i) \cap suA_\varphi(i) \neq preA_{\varphi'}(i))\,] \quad (9)$$

For each customer, the method checks whether the preceding and succeeding arcs differ between two individuals. If they do, the difference is marked as 1. Then, the Hamming distance $\xi(\varphi, \varphi')$ is averaged over all customers.

The diversity contribution $\Phi(\varphi)$ of an individual φ is determined by calculating the average Hamming distance of φ to its nearest individuals in the population as Eq. (10). The number of nearest individuals n_{close} is calculated as $n_{close} = nc \times n$ where nc is the proportion of nearest individuals, and n is the number of customers. $\mathcal{N}_{close}$ represents the set of nearest individuals.

$$\Phi(\varphi) = \frac{1}{n_{close}} \sum_{\varphi' \in \mathcal{N}_{close}} \xi(\varphi, \varphi') \quad (10)$$

The diversity contribution $\Phi(\varphi)$ quantifies how different an individual solution φ is from its closest neighbors in the population. This diversity measure helps to maintain population variety during the optimization process and prevents premature convergence.

3) Fitness Evaluation Function: To effectively assess the overall quality of a solution, we propose a comprehensive fitness evaluation function. This function integrates solution cost, constraint violation penalties, and diversity contribution.

Firstly, we explain the total quality function in Eq. (11). The total quality $\Psi(\varphi)$ of a solution φ is calculated by summing the total distance $TD(\varphi)$ and the total penalty $P(\varphi)$.

$$\Psi(\varphi) = TD(\varphi) + P(\varphi) \quad (11)$$

This function assesses the quality of a solution by considering both its efficiency (measured by total travel distance) and feasibility (penalizing constraint violations). A solution with a lower $\Psi(\varphi)$ is considered better, as it indicates lower cost and fewer constraint violations. Additionally, $\Psi(\varphi)$ is used in local search to evaluate the quality of neighboring solutions.

Next, we introduce two ranking functions $fit(\varphi)$ and $dc(\varphi)$ that rank the solutions based on their total quality and diversity contribution, respectively.

$$fit(\varphi) = rank(\Psi(\varphi)) \quad (12)$$

$$dc(\varphi) = rank(\Phi(\varphi)) \quad (13)$$

$fit(\varphi)$ ranks the solutions in the population in ascending order of $\Psi(\varphi)$, assigning lower values higher ranks to indicate better solutions. For example, the solution with the smallest $\Psi(\varphi)$ is ranked 1. Similarly, $dc(\varphi)$ ranks the solutions in descending order of $\Phi(\varphi)$, giving higher ranks to solutions with greater diversity, thereby promoting population diversity.

This ranking method mitigates the effects of differing units or scales, enhancing the stability of the optimization process.

Finally, the comprehensive fitness function adopts the biased fitness formulation proposed by Vidal *et al.* [21], as shown in Eq. (14). It is calculated by combining two ranking functions $fit(\varphi)$ and $dc(\varphi)$ for both total quality and diversity contribution, respectively. The number of elite individuals nbE is calculated as $nbE = el \times n$, where el is the proportion of elite individuals, and n is the number of customers. nbP is the total number of individuals in the population.

$$BiasedFitness(\varphi) = fit(\varphi) + \left(1 - \frac{nbE}{nbP}\right) \cdot dc(\varphi) \quad (14)$$

C. Efficient Local Search (ELS)

The efficient local search procedure comprises two main components. First, a Conditional AFS-Insert (CAI) rule is introduced, from which four new move operators are derived to effectively explore the solution neighborhoods. Second, a constant-time move evaluation mechanism is developed to significantly reduce the computational overhead during the search process. The details of these two components are provided in the following subsections.

To better understand the ELS procedure, we provide the pseudo-code in Algorithm 2. ELS starts by setting the current solution φ_a to solution φ_c (line 1). The algorithm iteratively improves the solution φ_a through neighborhood exploration (lines 2–7). It checks nine different move operators, N_1 to N_9 (see Section III-C1). Specifically, N_1 to N_4 represent insertion and swap-based move operators following the CAI rule, and for simplicity, we denote N_1 to N_4 as CAI move operators. N_5 to N_9 are the classic move operators that include swap-based, 2-opt, and inter-route 2-opt* move operators. For each N_i, the algorithm explores the best solution φ, starting from the current solution φ_a (line 4). The quality $\Psi(\varphi)$ and $\Psi(\varphi_a)$ are efficiently computed according to the constant-time move evaluation mechanism (see Section III-C2). If $\Psi(\varphi) < \Psi(\varphi_a)$, the algorithm updates φ_a to φ and restarts neighborhood exploration from the updated φ_a (lines 5-6). The loop of neighborhood exploration terminates once neighborhood exploration yields no further improvement (line 7). If φ_a is infeasible and with a certain probability P_{rep}[1], the *Repair* phase is triggered (line 8). In this phase, the penalty weights are temporarily increased tenfold, and neighborhood exploration is restarted from φ_a to get a new solution φ_b. Otherwise, φ_b is directly set to φ_a (line 11). Finally, the algorithm returns both solutions φ_a and φ_b (line 12).

1) Move Operators: Before introducing the move operators, we first introduce the Conditional AFS-Insert (CAI) Rule. The CAI Rule is a key mechanism that ensures the feasibility of move operators in ELS. Denote $minAFS$ as the AFS nearest to the preceding customer. The CAI Rule inserts the $minAFS$ only when the number of customers in the route increases and the route does not already contain any AFS. This insertion mechanism is integrated with regular

---

Algorithm 2: Efficient local search (ELS).

Input: Total quality function Ψ, solution φ_c and probability of executing the repair phase P_{rep}
Output: Solution φ_a and solution φ_b
/* Move operators: N_1–N_9 with CAI move operators N_1–N_4 and classic move operators N_5–N_9. */
/* *Repair*: temporarily increases penalty weights tenfold and restarts neighborhood exploration to fix infeasible solutions. */

1 $\varphi_a \leftarrow \varphi_c$;
  /* Start neighborhood exploration */
2 **repeat**
3   **for** $i \leftarrow 1$ **to** 9 **do**
4       $\varphi \leftarrow$ Best solution in N_i starting from φ_a;
        /* Evaluate quality using the constant-time move evaluation mechanism */
5   **if** $\Psi(\varphi) < \Psi(\varphi_a)$ **then**
6          $\varphi_a \leftarrow \varphi$, **break**;
7 **until** $\Psi(\varphi_a) < \Psi(\varphi)$;
  /* End neighborhood exploration */
  /* Start repair phase */
8 **if** φ_a is infeasible and with probability P_{rep} **then**
9    $\varphi_b \leftarrow Repair(\varphi_a)$
10 **else**
11    $\varphi_b \leftarrow \varphi_a$
12 **return** Solution φ_a and solution φ_b

---

move operators, leading to four CAI move operators. This conditional AFS insertion prevents cases the total distance $TD(\varphi)$ of discovered solution φ is reduced, yet an individual route exceeds D_{max}, rendering the move invalid. For example, consider two routes: (x_1, x_2, x_3) and (x_4, x_5, x_6). When attempting to insert customer x_1 after customer x_4, a traditional move operator would produce the route (x_4, x_1, x_5, x_6), which exceeds D_{max}. However, with the CAI Rule, the $minAFS$ is conditionally added, producing the feasible route $(x_4, x_1, minAFS, x_5, x_6)$.

In ELS, the move operators include CAI move operators N_1-N_4 and classic move operators N_5-N_9. For CAI move operators, N_1-N_3 are insertion-based, while N_4 is swap-based. For classic move operators, N_5-N_6 are swap-based, involving the exchange of two arcs. N_7 uses the intra-route 2-opt operator. N_8 and N_9 apply the inter-route 2-opt* operator, differing in the number of paths. After each move operator is applied, METS removes any AFS whose deletion does not result in a violation of the maximum driving range limit D_{max}.

Before we introduce the move operators in details, we first provide the following definitions. Let $r(x)$ be the route r that includes the customer x, and let (x_i, x_j) denote a partial route from x_i to x_j. Denote y as the α-th closest customer of x where $\alpha = \max\{5, \lceil 5\% \cdot n \rceil\}$ and n is the total number of customers [35]. Let x' and y' be the nodes following x and y, respectively.

CAI move operators $N_1 - N_4$

- $CAI\text{-}Insert$ (N_1): Remove x and place x after y. If $r(y)$ does not include an AFS, add $minAFS$ after x.
- $CAI\text{-}Insert\text{-}Arc$ (N_2): If x' is a customer, remove x and x', then place x and x' after y. When $r(x) \neq r(y)$ and $r(y)$ does not include an AFS, add $minAFS$ after

---

[1]In this paper, we set $P_{rep} = 0.5$.

x'.

- $CAI\text{-}Insert\text{-}ReversedArc$ (N_3): If x' is a customer, remove x and x', then place x' and x after y. When $r(x) \neq r(y)$ and $r(y)$ does not include an AFS, add $minAFS$ after x.
- $CAI\text{-}Swap\text{-}Arc$ (N_4): If x' is a customer, swap x and x' with y. When $r(x) \neq r(y)$ and $r(y)$ does not include an AFS, add $minAFS$ after x'.

Classic move operators $N_5 - N_9$

- $Swap$ (N_5): Swap x and y.
- $Swap\text{-}DoubleArcs$ (N_6): If x' and y' are customers, swap x and x' with y and y.
- $2\text{-}opt$ (N_7): If $r(x) = r(y)$, replace (x, x') and (y, y') with (x, y) and (x', y').
- $2\text{-}opt^*\text{-}DoublePaths$ (N_8): If $r(x) \neq r(y)$, replace (x, x') and (y, y') with (x, y) and (x', y').
- $2\text{-}opt^*\text{-}TriplePaths$ (N_9): If $r(x) \neq r(y)$, replace (x, x') and (y, y') with (x, y') and (x', y).

2) Constant-Time Move Evaluation: For efficient neighborhood evaluations, we implement a fast move evaluation technique supported by a data structure. This technique allows neighboring solutions to be evaluated in constant time, enabling quick evaluations of routes during the local search. Specifically, a Customer-Relative-AFS (CRA) data structure is a one-dimensional array of length n to record the relative positions of customers and AFS, where n is the number of customers. To calculate the relative positions in a route, set $CRA(x) = -1$ when customer x is visited before the AFS or if there is no AFS, and set $CRA(x) = 1$ is visited after the AFS. **Proposition 1** presents the time complexities of evaluating neighboring solutions and exploring the complete neighborhood, with the proof provided in the supplementary.

Proposition 1. In METS, for all moves operators N_1-N_9, the time complexity of evaluating neighboring solution is $O(1)$. Let n be the number of customers and α be the number of neighboring nodes for each customer. For each move, the time complexity of evaluating exploring the complete neighborhood is $O(\alpha n)$.

D. Overall Framework of METS

This subsection presents the overall framework of METS as presented in Algorithm 3. METS begins by generating an initial population P using $SCTS$ and records the current best solution φ^* (lines 1–2). The algorithm proceeds to the main search process (lines 3–19) and continues until the termination conditions are met. In the main search process, parent selection employs binary tournament selection based on $BiasedFitness$ to choose φ_1 and φ_2 from both feasible and infeasible subpopulations (line 4). Subpopulations are explicitly defined based on solution feasibility to better manage diversity and feasibility. Moreover, $\Phi(\varphi)$, $fit(\varphi)$ and $dc(\varphi)$ are evaluated independently within each subpopulation (see Section III-B). The Order Crossover operator[2] [34] is applied

---

[2]The Order Crossover operator randomly selects a subsequence from one parent and copies it into the offspring. The remaining positions are filled based on the order of genes in the other parent. This method preserves the relative order of genes and generates effective solutions.

Algorithm 3: METS

> **Input:** Input graph $G(V, E)$, total quality function Ψ, lower bound of subpopulation μ, upper bound of subpopulation λ, maximum allowed number of iterations $MaxIter$, maximum allowed number of iterations without improvement It_{NI}, maximum allowed time $Maxtime$, repair probability parameter P_{rep} and penalty adjust parameter NS
> **Output:** Best found solution φ^*
> /* $SCTS$ represents separate constraint-based tour split strategy. */
> /* TSP represents a set of random sequences containing all customers. */
> /* ELS represents efficient local search. */
> /* $SelectSurvivors$ represents the process to maintain the quantity of population. */

1   $Initial\ population = \{\varphi_1, ...\varphi_p\} \leftarrow SCTS(TSP)$;
2   $\varphi^* \leftarrow \arg\min\{\Psi(\varphi_i), i = 1, \ldots, N_p\}$;
3   **while** $MaxIter$, It_{NI}, and $Maxtime$ are not reached **do**
4   Select parent solutions φ_1 and φ_2;
5   Produce a giant tour offspring C from φ_1 and φ_2;
6      $\varphi_c \leftarrow SCTS(C)$;
7      $(\varphi_a, \varphi_b) \leftarrow ELS(\varphi_c)$;
8   **if** $\varphi_a = \varphi_b$ **then**
9   Insert φ_a into a subpopulation based on feasibility;
10   **else**
11   Insert φ_a and φ_b into subpopulations based on their respective feasibility;
12   Update subpopulations $BiasedFitness$;
13   **if** subpopulation size reached λ **then**
14         $P \leftarrow SelectSurvivors(P)$;
15   **if** $\Psi(\varphi_b) < \Psi(\varphi^*)$ **then**
16         $\varphi^* \leftarrow \varphi_b$;
17   **if** number of iterations mod $NS = 0$ **then**
18   Adjust penalty parameters ω^T, ω^D and ω^C;
19   Update infeasible subpopulation's $BiasedFitness$;
20 **return** Best found solution φ^*

---

to generate a giant tour C from the parent solutions (line 5). Then, METS converts the giant tour C into a solution φ_c using the $SCTS$ (line 6). Subsequently, φ_c is refined through efficient local search, producing two improved solution φ_a and φ_b (line 7). If $\varphi_a = \varphi_b$, only φ_a is inserted into the subpopulation based on its feasibility (lines 8-9). Otherwise, φ_a and φ_b are inserted into the subpopulations based on their respective feasibility (lines 10-11).

Next, update the $BiasedFitness$ of subpopulations (line 12). When upper bound λ is reached, the $SelectSurvivors$ procedure is triggered to maintain the subpopulation size within a reasonable range. $SelectSurvivors$ iteratively removes individuals, prioritizing cloned solutions and those with worse $BiasedFitness$, until the subpopulation size reaches the lower bound μ (lines 13–14).

If $\Psi(\varphi_b)$ is better than $\Psi(\varphi^*)$, φ_b replaces φ^* as the best solution (lines 15–16). This comparison is made only between φ_b and the current best solution φ^*. Since φ_b is either identical to φ_a or derived from φ_a through the repair phase, it is always as good as or better than φ_a. Every $NS = 20$ iterations, the penalty parameters are adjusted based on the percentage of solutions that satisfy each constraint. If any rate is $\leq$ 15%, indicating that the penalty is too light, the corresponding

penalty is increased by 20%. Conversely, if any rate is $\geq 25\%$, indicating that the penalty is too strict, it is decreased by 15%. The $BiasedFitness$ of infeasible individuals is then updated according to the adjusted penalty parameters (lines 17–19). Finally, METS returns the best feasible solution φ^* (line 20).

IV. COMPUTATIONAL STUDIES

The effectiveness of METS is evaluated through comprehensive comparisons with recent approaches for solving GVRP-PCAFS on existing public benchmark sets containing small-scale (15 customers) and medium-scale (25 to 100 customers) instances. Additionally, a new large-scale benchmark set named Beijing is introduced, containing instances ranging from 200 to 1000 customers based on real-world logistics data collected from the city, to better reflect practical scenarios. Both METS and GRASP are tested on the Beijing set and their results are reported. Finally, investigations are conducted to validate the effectiveness of three key components in METS, i.e., the SCTS strategy, the comprehensive fitness evaluation function, and the efficient local search procedure with its new move operators and evaluation mechanism. The source code of METS and the new benchmark set are open-sourced anonymously at https://anonymous.4open.science/r/METS-D7B4.

A. Experimental Setup

1) Benchmark Sets: The experiments are conducted on three benchmark sets. The first two sets, named CENTRAL set and Large-sized CENTRAL set, are originally proposed by Bruglieri *et al.* [8]. For clarity, these sets are renamed as S-Central and M-Central in this article. The third set, named Beijing, is newly introduced based on real-world logistics data.

- **S-Central Set.** This set contains 10 small-scale instances with 15 customers each. In each instance, a single AFS is located at the center of the customer area with a capacity of one AFV. The depot is positioned two hours away from the AFS. Each instance allows up to 15 available AFVs, with a route duration limit of seven hours and a maximum driving range of 160 miles. AFVs travel at 40 miles per hour, with both customer service time and refueling time set to 0.5 hours.
- **M-Central Set.** This set contains 30 medium-scale instances, divided into three groups of 10 instances each with 25, 50, and 100 customers respectively. The AFS capacity increases with problem size: two AFVs for 25-customer instances, three for 50-customer instances, and eight for 100-customer instances. The maximum number of available AFVs is set to 7, 13, and 25 for 25, 50, and 100-customer instances, respectively. All instances have the same route duration limit of 7.5 hours and maintain the same vehicle speed, service time, and refueling time as the S-CENTRAL set.
- **Beijing Set.** This new set is created based on data from the JD Logistics company in Beijing, China. The original collected data contains 3000 delivery requests over several days in the city. From this dataset, 20 large-scale instances are generated through sampling, with customer sizes being 200, 400, 600, 800, and 1000 (4 instances per

TABLE I
DESCRIPTION AND RANGES OF THE PARAMETERS OF METS USED FOR
AUTOMATIC PARAMETER TUNING WITH IRACE [36].

Parameter	Description	Type	Value Range	Value
ω^T	Overtime penalty parameter	Integer	[1, 1000]	527
ω^D	Over-mileage penalty parameter	Integer	[1, 1000]	430
ω^C	Over-capacity penalty parameter	Integer	[1, 1000]	195
μ	lower bound of subpopulation size	Integer	[5, 200]	154
λ	upper bound of subpopulation size	Integer	[10, 400]	222
el	Proportion of elite individuals	Real	(0,1)	0.5
nc	Proportion of close individuals	Real	(0.1)	0.2

size). The AFS capacity increases with problem size: 20, 40, 60, 80, and 100 AFVs for 200, 400, 600, 800, and 1000-customer instances, respectively. The locations of customers, depot, and AFSs are specified using latitude and longitude coordinates, and the distances between them are calculated as the Euclidean distance. The route duration limit is set to 8 hours, with no strict limit on the number of available AFVs. The vehicle speed, service time and refueling time remain the same as the previous two sets.

2) Compared Methods and Parameter Settings: METS is compared with the state-of-the-art methods for solving GVRP-PCAFS, including the exact method CP-Proactive [7] and the heuristic algorithm GRASP [8]. Compared to CP-Proactive that is restricted to small-scale instances, GRASP has better scalability as it can find high-quality solutions for medium-scale instances within reasonable computational time. Hence, GRASP is the primary compared algorithm in the experiments. As the original GRASP code is unavailable, both algorithms are implemented in Matlab for fair comparison. The original GRASP implementation used a 2-minute time limit as the termination condition. We find that for instances with 15 and 25 customers, GRASP typically converges well before this time limit. However, for instances with 50 and 100 customers, GRASP is far from convergence within 2 minutes. Therefore, to ensure sufficient convergence, both GRASP and METS are set to terminate when the maximum number of iterations reaches 2000 or when 300 consecutive iterations show no improvement. For parameter settings in METS, the population management parameters el and nc are set to 0.5 and 0.2, respectively, based on recommended settings from existing EAs for solving VRPs that incorporate similar population control mechanisms [21]. The remaining parameters are then tuned using the automatic parameter tuning tool irace [36]. The training set consists of 10 randomly selected problem instances from all 60 test instances, with the tuning budget (maximum number of algorithm runs during tuning) set to 2000. The parameters and their final values are summarized in Table I. The number of subpopulations ranges from μ to λ. These values are also recommended for future research when METS is employed, since METS with such setting demonstrates good performance across all three benchmark sets in the experiments. For fair comparison, GRASP also undergoes the same tuning procedure for its parameter β, which influences the solution construction process. The tuned

TABLE II
COMPARATIVE RESULTS BETWEEN METS AND REFERENCE ALGORITHMS ON SMALL-SCALE INSTANCES THE IN S-CENTRAL SET. FOR EACH INSTANCE, THE BETTER PERFORMANCE IS INDICATED IN BOLD, NEW BEST-KNOWN SOLUTIONS (BKSs) ARE HIGHLIGHTED IN GRAY, AND RESULTS SIGNIFICANTLY BETTER THAN GRASP, BASED ON 30 INDEPENDENT RUNS, ARE MARKED WITH UNDERLINES ACCORDING TO THE WILCOXON SIGNED RANK TEST AT A SIGNIFICANCE LEVEL OF p-VALUES < 0.05

Instance	CP-Proactive	GRASP				METS			Imp. B (%)	Imp. A (%)	p-value
	Best [7]	Best [8]	Best	Average	Time (s)	Best	Average	Time (s)			
S-Central_1	**953.94**	**953.94**	**953.94**	955.85	8.15	**953.94**	953.94	17.63	0.00%	-0.20%	2.54E-4
S-Central_2	**948.69**	959.88	959.88	963.95	23.05	959.88	959.88	16.24	0.00%	-0.42%	2.49E-6
S-Central_3	**943.12**	958.94	958.94	967.09	28.09	958.94	959.24	19.43	0.00%	-0.81%	2.50E-6
S-Central_4	967.96	1099.24	1098.49	1128.93	56.37	947.98	1086.91	27.66	-13.76%	-3.72%	1.72E-6
S-Central_5	**714.55**	**714.55**	**714.55**	714.55	1.74	**714.55**	714.55	9.68	0.00%	0.00%	1.00E-0
S-Central_6	**844.43**	**844.43**	845.53	863.22	2.29	**844.43**	844.43	17.35	0.00%	-2.18%	1.73E-6
S-Central_7	**862.68**	**862.68**	867.78	888.24	1.76	**862.68**	862.68	14.59	0.00%	-2.88%	1.73E-6
S-Central_8	**712.83**	**712.83**	**712.83**	723.29	1.14	**712.83**	712.83	21.05	0.00%	-1.45%	3.77E-6
S-Central_9	**855.43**	**855.43**	**855.43**	874.88	1.34	**855.43**	855.43	1.89	0.00%	-2.22%	5.55E-6
S-Central_10	**901.19**	905.59	905.59	924.57	2.43	905.59	906.23	11.35	0.00%	-1.98%	2.56E-6
No. Best	9	6	4			7					
Mean / W-D-L	870.48	886.75	887.30	900.46	12.64	871.63	885.61	15.69	-1.38%	-1.59%	9-1-0

value for β is 0.23, which is then used in the experiments.

3) Evaluation Metrics: For small and medium-scale instances, both METS and GRASP are executed 30 independent times. The best and average solution quality across these runs are reported. In each run, the time to find the best solution (time-to-best) is recorded, and the average of time-to-best across 30 runs is reported for both algorithms. For the large-scale instances in the Beijing set, to prevent prohibitively long runtime, both GRASP and METS are set a maximum runtime of 7200s. Due to the extensive computational requirements on these large-scale instances, both algorithms are executed 10 independent times on them. For CP-Proactive, the solution quality results reported in the original paper [7], which were obtained with a maximum runtime of 3600s, are directly obtained and included in this article. All the experiments are conducted in Matlab (version 2022a) on the same machine with Intel Core i5-12500H, 3.1 GHz, 24 GB RAM.

B. Results on Small, Medium, and Large-Scale Instances

Tables II-IV present the comparative results on the S-Central, M-Central, and Beijing benchmark sets, respectively. A brief description of the contents in the tables is given below.

- For both METS and GRASP, columns headed "Best" and "Average" report the best and average solution quality in terms of TD across the repeated runs, while the "Time" column shows the average time-to-best. Since GRASP found most of the current best-known solutions (BKSs) for instances in the M-Central set, the best results reported in the original GRASP paper are included in Tables II and III for comparison, with columns being indicated by the corresponding citation [8].

- The columns "Imp. B" and "Imp. A" report the improvement ratios achieved by METS compared to GRASP in terms of best solution quality and average solution quality, respectively. These ratios are calculated by taking the difference between METS's result and GRASP's result, then divided by GRASP's result. Therefore, negative

ratios indicate that METS improves upon GRASP (i.e., reducing the solution cost), with larger absolute values of ratios representing greater improvements.

- The "p-value" columns in these tables report the statistical significance based on the Wilcoxon rank-sum test when comparing the average solution quality of METS and GRASP. Results are considered statistically significant when $p < 0.01$, and these significant better results are underlined in the tables.

- For CP-Proactive, the solution quality results obtained with maximum runtime of 3600s from the original paper are presented in Table II, indicated by the corresponding citation [7]. This method is omitted in Table III and IV as it typically cannot find solutions within reasonable time for medium and large-scale instances.

- In the last two rows of these tables, "No. Best" shows the number of instances in the benchmark set where an algorithm achieves the best solution quality. "Mean / W-D-L" presents the mean values across all instances for each metric. For the "p-value" column, the "Mean / W-D-L" row shows the win-draw-loss (W-D-L) counts of the statistical comparison between METS and GRASP, indicating the number of instances where METS performs significantly better, shows no significant difference, or performs significantly worse than GRASP.

- For each instance, the best solution quality among all "Best" columns is indicated in bold. **New** BKSs that improve uopon the previous ones are highlighted in gray.

From Tables II-IV, the effectiveness of METS can be evaluated from two aspects, i.e., best solution quality and average solution quality. Regarding best solution quality, METS obtains the best solutions on 57 out of 60 GVRP-PCAFS instances, which is significantly better than the compared algorithms. Specifically, for all 30 medium-scale instances (Table III), METS discovers new BKSs across all of them over the previous ones found by GRASP. The improvement ratios in these new BKSs over previous ones are considerable, with

TABLE III
COMPARATIVE RESULTS BETWEEN GRASP AND METS ON MEDIUM-SCALE INSTANCES. FOR EACH INSTANCE, THE BETTER PERFORMANCE IS INDICATED IN BOLD, NEW BEST-KNOWN SOLUTIONS ARE HIGHLIGHTED IN GRAY, AND RESULTS SIGNIFICANTLY BETTER THAN GRASP, BASED ON 30 INDEPENDENT RUNS, ARE MARKED WITH UNDERLINES ACCORDING TO THE WILCOXON SIGNED RANK TEST AT A SIGNIFICANCE LEVEL OF P-VALUES< 0.05

Instance	GRASP				METS			Imp. B (%)	Imp. A (%)	p-value
	Best [8]	Best	Average	Time (s)	Best	Average	Time (s)			
M-Central25_1	1129.85	1135.96	1152.87	30.59	**1129.71**	1129.71	34.02	-0.01%	-2.01%	1.73E-6
M-Central25_2	1113.97	1118.35	1136.12	21.73	**1113.80**	1113.80	22.64	-0.02%	-1.96%	1.73E-6
M-Central25_3	1321.82	1324.64	1344.36	126.47	**1320.27**	1320.27	4.88	-0.12%	-1.79%	1.73E-6
M-Central25_4	1122.73	1126.69	1140.37	30.23	**1118.87**	1121.38	34.51	-0.34%	-1.67%	1.73E-6
M-Central25_5	1110.36	1122.85	1140.74	24.47	**1109.55**	1109.57	20.37	-0.07%	-2.73%	1.73E-6
M-Central25_6	1090.04	1092.91	1118.17	7.29	**1089.92**	1089.92	4.10	-0.01%	-2.53%	1.73E-6
M-Central25_7	1105.04	1112.69	1133.56	17.98	**1103.82**	1103.82	15.79	-0.11%	-2.62%	1.73E-6
M-Central25_8	1141.23	1137.81	1216.42	31.93	**1134.93**	1137.60	42.67	-0.55%	-6.48%	1.73E-6
M-Central25_9	1281.57	1288.38	1303.99	30.11	**1275.57**	1280.19	20.03	-0.47%	-1.83%	1.73E-6
M-Central25_10	1311.67	1320.85	1337.36	53.88	**1311.53**	1311.53	3.48	-0.01%	-1.93%	1.73E-6
M-Central50_1	2520.33	2498.19	2529.29	587.29	**2441.41**	2461.88	94.88	-3.13%	-2.66%	1.73E-6
M-Central50_2	2435.78	2413.48	2461.84	1112.44	**2241.35**	2345.87	116.12	-7.98%	-4.71%	1.73E-6
M-Central50_3	2425.64	2268.80	2411.91	620.75	**2230.13**	2239.30	153.98	-8.06%	-7.16%	1.73E-6
M-Central50_4	2271.14	2257.60	2332.61	426.97	**2193.74**	2200.93	116.19	-3.41%	-5.65%	1.73E-6
M-Central50_5	2467.29	2453.61	2490.11	686.60	**2393.32**	2403.36	66.45	-3.00%	-3.48%	1.73E-6
M-Central50_6	2422.87	2446.28	2472.57	583.80	**2380.99**	2388.86	114.55	-1.73%	-3.39%	1.73E-6
M-Central50_7	2405.19	2262.98	2414.30	777.76	**2221.61**	2241.80	169.11	-7.63%	-7.14%	1.73E-6
M-Central50_8	2487.32	2474.34	2518.88	779.13	**2415.43**	2421.01	149.28	-2.89%	-3.89%	1.73E-6
M-Central50_9	2450.04	2409.39	2460.41	648.02	**2241.03**	2370.72	117.36	-8.53%	-3.65%	1.73E-6
M-Central50_10	2473.63	2436.74	2484.88	682.37	**2402.03**	2407.71	100.30	-2.89%	-3.11%	1.73E-6
M-Central100_1	4966.03	4766.64	4932.28	1281.24	**4645.27**	4666.38	495.11	-6.46%	-5.39%	1.73E-6
M-Central100_2	4730.11	4673.30	4784.78	1743.75	**4479.99**	4556.14	411.37	-5.29%	-4.78%	1.73E-6
M-Central100_3	4757.50	4527.97	4736.68	1618.37	**4447.56**	4498.85	738.21	-6.52%	-5.02%	1.73E-6
M-Central100_4	4697.35	4452.41	4604.47	1036.62	**4257.75**	4351.95	470.07	-9.36%	-5.48%	1.73E-6
M-Central100_5	4732.49	4681.76	4766.02	1254.83	**4465.08**	4552.13	445.71	-5.65%	-4.49%	1.73E-6
M-Central100_6	4524.44	4468.79	4528.98	983.92	**4257.08**	4370.95	527.36	-5.91%	-3.49%	1.73E-6
M-Central100_7	4786.57	4558.80	4786.81	1166.55	**4462.69**	4559.14	428.45	-6.77%	-4.76%	1.73E-6
M-Central100_8	4784.18	4507.96	4750.78	923.39	**4436.81**	4450.38	751.02	-7.26%	-6.32%	1.73E-6
M-Central100_9	4795.70	4705.49	4814.19	1154.06	**4507.85**	4603.30	403.65	-6.00%	-4.38%	1.73E-6
M-Central100_10	4686.57	4496.40	4605.44	892.67	**4366.85**	4372.59	477.49	-6.82%	-5.06%	1.73E-6
No. Best	0	0			30					
Mean / W-D-L	2784.95	2718.07	2797.04	644.51	2639.86	2672.70	218.30	-3.90%	-3.98%	30-0-0

METS achieving an average improvement of 1.38% compared to GRASP. This observation extends to the 20 large-scale instances (Table IV), where METS finds the best solutions across all instances with an even larger average improvement ratio of 3.90% compared to GRASP. For small-scale instances, METS achieves slightly fewer best solutions compared to CP-Proactive, which is reasonable given CP-Proactive's nature as an exact method. However, in the original paper [7], CP-Proactive executes under a maximum runtime of 3600s, and solutions returned at this time limit are not guaranteed to be optimal due to early termination. This situation occurs on instances S-Central_3 and S-Central_4. Notably, for S-Central_4, METS discovers a new BKS that improves upon the solution found by CP-Proactive. Compared to GRASP, METS maintains its advantage by finding more best solutions and achieving an average improvement ratio of 1.38% in best solution quality.

In terms of average solution quality, METS demonstrates significantly better performance than GRASP on 59 out of 60 instances, with only one exception in the S-Central set. The improvements are substantial across all problem sizes, with average improvement ratios of 1.59%, 3.98%, and 3.43%

for small, medium, and large-scale instances, respectively. In summary, these results validate the effectiveness of METS, as it achieves improvements over existing methods in both best and average solution quality, by a large margin. Finally, regarding time-to-best, METS and GRASP show comparable average results for small and large-scale instances, while METS demonstrates a clear advantage for medium-scale instances. Considering that METS consistently finds solutions of higher quality than GRASP, it can be concluded that METS has higher search efficiency than GRASP. This advantage is likely due to the efficient local search procedure in METS, particularly its move evaluation mechanism, which will be further analyzed in Section IV-C.

C. Effectiveness of the New Move Operators and Constant-Time Move Evaluation

To verify the effectiveness of the efficient local search design in METS, we conducted ablation experiments evaluating the impact of CAI-based move operators and the constant-time move evaluation mechanism. Due to the prohibitive computational time on large-scale instances, these experiments

TABLE IV
COMPARATIVE RESULTS BETWEEN GRASP AND METS ON LARGE-SCALE INSTANCES. FOR EACH INSTANCE, THE BETTER PERFORMANCE IS INDICATED IN BOLD, NEW BEST-KNOWN SOLUTIONS ARE HIGHLIGHTED IN GRAY, AND RESULTS SIGNIFICANTLY BETTER THAN GRASP, BASED ON 10 INDEPENDENT RUNS, ARE MARKED WITH UNDERLINES ACCORDING TO A NON-PARAMETRIC TEST AT A SIGNIFICANCE LEVEL OF P-VALUES < 0.05.

Instance	GRASP			METS			Imp. B (%)	Imp. A (%)	p-value
	Best	Average	Time (s)	Best	Average	Time (s)			
Beijing200_1	4501.82	4625.52	744.67	**4371.96**	4471.99	793.31	-2.88%	-3.32%	1.95E-3
Beijing200_2	6427.97	6518.65	1715.03	**6334.57**	6338.20	468.90	-1.45%	-2.77%	1.95E-3
Beijing200_3	4534.42	4641.68	859.02	**4408.75**	4517.95	1150.40	-2.77%	-2.67%	1.95E-3
Beijing200_4	6638.99	6661.33	3059.21	**6407.07**	6421.63	957.12	-3.49%	-3.60%	1.95E-3
Beijing400_1	8555.42	8806.39	2750.79	**8530.72**	8540.35	3599.28	-0.29%	-3.02%	1.95E-3
Beijing400_2	12561.23	12832.85	1338.38	**12277.58**	12363.36	5394.36	-2.26%	-3.66%	1.95E-3
Beijing400_3	8894.16	9078.44	3554.22	**8759.47**	8776.04	2943.84	-1.51%	-3.33%	1.95E-3
Beijing400_4	12827.50	12859.35	5794.46	**12534.83**	12541.83	3177.82	-2.28%	-2.47%	2.50E-4
Beijing600_1	12973.91	13107.71	3842.63	**12499.83**	12635.17	2642.80	-3.66%	-3.61%	1.95E-3
Beijing600_2	19045.21	19098.85	1713.12	**18216.44**	18230.19	3030.78	-4.35%	-4.55%	1.95E-3
Beijing600_3	13480.33	13637.78	4030.21	**12971.00**	13004.98	3062.95	-3.78%	-4.64%	1.95E-3
Beijing600_4	19590.56	19624.95	3718.51	**18729.00**	18741.17	3544.35	-4.40%	-4.50%	3.03E-2
Beijing800_1	17202.25	17278.42	4132.25	**16639.33**	16698.09	3249.93	-3.27%	-3.36%	1.95E-3
Beijing800_2	25256.34	25429.95	2619.32	**24339.56**	24350.28	3654.35	-3.63%	-4.25%	1.95E-3
Beijing800_3	17693.31	17901.67	4555.37	**17160.56**	17251.10	2911.35	-3.01%	-3.63%	1.95E-3
Beijing800_4	25818.11	25905.35	2846.25	**24895.48**	25003.68	4323.42	-3.57%	-3.48%	3.03E-2
Beijing1000_1	21200.92	21434.34	4630.98	**20660.36**	20930.28	3564.84	-2.55%	-2.35%	1.95E-3
Beijing1000_2	31259.10	31413.30	5972.08	**30263.36**	30320.29	3017.30	-3.19%	-3.48%	1.95E-3
Beijing1000_3	21972.00	22204.79	2580.45	**21353.74**	21507.25	4614.13	-2.81%	-3.14%	1.95E-3
Beijing1000_4	32182.91	32201.06	6170.15	**31237.51**	31278.36	4872.71	-2.94%	-2.87%	1.03E-4
No. Best	0			20					
Mean / W-D-L	16130.82	16263.12	3331.36	15629.53	15696.11	3048.70	-2.91%	-3.43%	20-0-0

focused on instances with up to 100 customers, as the results already demonstrated clear benefits of these components.

TABLE V
RESULTS OF METS-WNM AND METS ON SMALL-SCALE AND MEDIUM-SCALE INSTANCES. EACH INSTANCE WAS SOLVED 30 TIMES AND THE ALGORITHM TERMINATES WHEN THE MAXIMUM NUMBER OF ITERATIONS REACHES 2000 OR WHEN THERE HAVE BEEN 300 CONSECUTIVE ITERATIONS WITHOUT IMPROVEMENT. THE BETTER PERFORMANCE IS INDICATED IN BOLD, AND RESULTS THAT ARE SIGNIFICANTLY BETTER THAN METS-WNM ARE MARKED WITH UNDERLINES ACCORDING TO THE WILCOXON SIGNED RANK TEST AT A SIGNIFICANCE LEVEL OF P-VALUES < 0.05.

Size	METS-WNM		METS		Imp. A (%)	W-D-L
	Average	Time (s)	Average	Time (s)		
15	916.83	26.80	**885.61**	15.69	-3.41%	10-0-0
25	1177.53	81.92	**1171.78**	20.25	-0.49%	10-0-0
50	2407.07	310.18	**2348.14**	119.82	-2.45%	10-0-0
100	4546.55	1155.54	**4498.18**	514.84	-1.06%	10-0-0
Mean	2262.00	393.61	2225.93	167.65	-1.59%	

To validate the effectiveness of the newly introduced moves, a variant algorithm METS-WNM was created that differs from METS in two aspects: (1) removal of the CAI rule, and (2) addition of a standard move operator that inserts AFS at the position with minimum additional cost in routes. Table V presents the comparative results between METS and METS-WNM in terms of average solution quality and time-to-best across 30 repeated runs. For each problem size, the improvement ratio (Imp. A) reports the average percentage improvement of METS over METS-WNM. The "W-D-L" columns indicate the number of instances where METS performed

significantly better, showed no significant difference, or performed significantly worse than METS-WNM, respectively. The results demonstrate that the CAI-based move operators consistently contribute to METS's performance. Specifically, METS significantly outperformed METS-WNM across all problem sizes and instances, achieving an average improvement ratio of 1.59%. For a deeper analysis, we ran both METS and METS-WNM 30 Time (s)s on four representative challenging instances (M-Central50_3, M-Central50_8, M-Central100_2, and M-Central100_4). The convergence charts in Figure 4 show that METS consistently outperforms METS-WNM across all iterations. Both algorithms reduce the objective value quickly within the first 2000 iterations. However, METS maintains a clear advantage throughout the process, delivering better solutions at every stage.

TABLE VI
RESULTS OF METS-WFAST AND METS ON SMALL-SCALE AND MEDIUM-SCALE INSTANCES. EACH INSTANCE WAS SOLVED 30 TIMES, THE CUT-OFF TIME WAS SET TO BE TEN TIMES THE NUMBER OF CUSTOMERS. THE BETTER PERFORMANCE IS INDICATED IN BOLD, AND RESULTS THAT ARE SIGNIFICANTLY BETTER THAN METS-WFAST ARE MARKED WITH UNDERLINES ACCORDING TO THE WILCOXON SIGNED RANK TEST AT A SIGNIFICANCE LEVEL OF P-VALUES < 0.05.

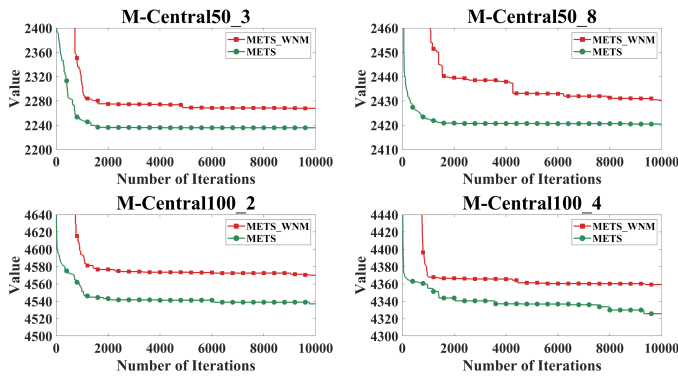| Size	METS-Wfast		METS		Imp. A (%)	W-D-L
	Average	Time (s)	Average	Time (s)		
15	893.41	33.17	**891.94**	13.59	-0.16%	0-10-0
25	1178.14	46.88	**1177.05**	22.37	-0.09%	0-10-0
50	2369.85	221.62	**2358.90**	144.38	-0.46%	4-6-0
100	4540.04	481.43	**4513.70**	435.68	-0.58%	6-4-0
Mean	2245.36	195.78	2235.40	154.01	-0.44%	

Fig. 4. The charts show the convergence profiles of METS-WNM and METS on the M-Central50_3, M-Central50_8, M-Central100_2, and M-Central100_4 instances across 30 independent runs. The lines represent the average best values with respect to the number of iterations.
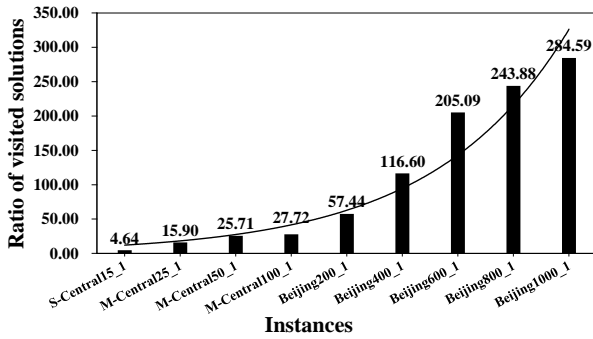

Fig. 5. The average ratio of the visited solutions of METS to METS-Wfast was calculated for nine instances of different sizes.

To evaluate the effectiveness of constant-time move evaluation, another variant METS-Wfast was created that excludes the fast evaluation mechanism. Since fast evaluation aims to accelerate the assessment of neighboring solutions, both algorithms were given a time limit of 10 times the number of customers as the termination condition. Table VI presents the comparative results following the same format as Table V. The results align with expectations - METS achieved improvements over METS-Wfast across all problem sizes, attributed to its ability to evaluate more solutions within the same time frame. For smaller instances with 15 and 25 customers, the inherent search capability of the algorithm masked the efficiency loss from removing fast evaluation, resulting in statistically insignificant differences. However, as problem size increased, the benefits of fast evaluation became more pronounced. METS showed statistically significant advantages in 4 out of 10 instances for 50-customer problems and 6 out of 10 instances for 100-customer problems. Figure 5 further illustrates this trend by comparing the number of neighboring solutions visited by both algorithms on nine instances of varying sizes. METS consistently evaluated more neighboring solutions than METS-Wfast, with the advantage growing more substantial as instance size increased, confirming the significant efficiency enhancement provided by the fast evaluation technique.
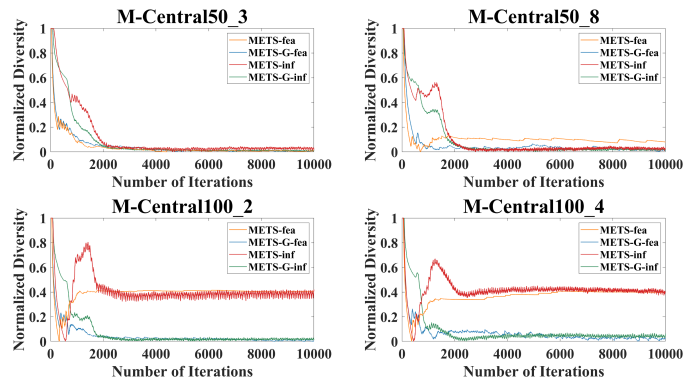

Fig. 6. The charts show the convergence profiles of METS and METS-G on four representative instances in terms of normalized average subpopulation diversity. The lines represent the average diversity of individuals in each subpopulation, normalized using min-max scaling within each instance. Each algorithm maintains two types of subpopulations: feasible (fea) and infeasible (inf). Higher values reflect greater population diversity during the search process.

D. A Deeper Look into the Dynamics of Diversity and Feasibility

To analyze how METS balances diversity and feasibility, we examined its convergence profiles on four representative instances, focusing on the dynamics of both aspects. Each instance was independently run 30 times, and the results are shown in Fig. 7 and Fig. 6, respectively.

To evaluate the effectiveness of the SCTS strategy in contribution of diversity, a variant algorithm, METS-G, was created by replacing SCTS with the construction phase of GRASP [8]. Fig. 6 shows the normalized diversity dynamics of feasible and infeasible subpopulations for METS and METS-G. At each iteration, the diversity of a subpopulation is calculated as the average of individual diversity values, computed using Eq. (10) and normalized via min-max scaling within each instance. METS consistently maintains higher diversity levels, especially in the infeasible subpopulation during the early and middle stages, demonstrating the advantage of SCTS in generating diverse offspring.

Fig. 7 presents the feasibility violation differences in the last 20 individuals across four representative instances. These individuals are selected to assess whether the adaptive adjustment of penalty weights and the comprehensive fitness function can effectively control constraint violations during the global search process in METS. For each constraint type (i.e., over-mileage, overtime, and over-capacity), the violation difference represents the average of difference between the number of feasible and infeasible individuals. As shown in the charts, all three constraints are well controlled, with violation differences quickly converging and fluctuating around zero. This confirms that METS can guide the population efficiently toward feasible regions while maintaining overall constraint satisfaction.

In summary, the experimental results demonstrate that METS effectively maintains a balance between population diversity and solution feasibility throughout the search process.
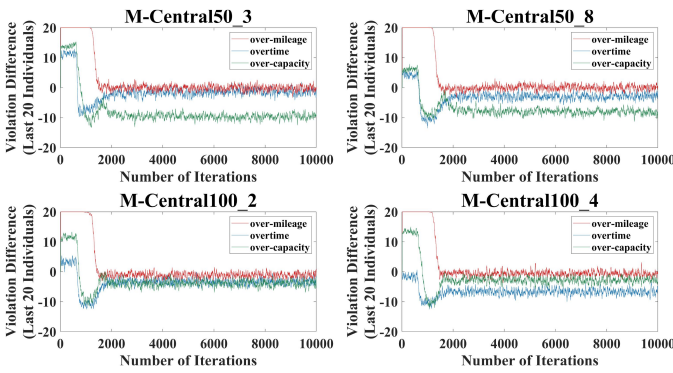
Fig. 7. The charts show the convergence profiles of METS on four representative instances in terms of feasibility violation difference. The lines represent the average of difference between the number of feasible and infeasible individuals among the last 20 individuals for each constraint type: overtime, over-mileage, and over-capacity. Positive values indicate more feasible individuals.

V. CONCLUSION

In this work, a novel memetic algorithm, dubbed METS, is proposed to solve the Green Vehicle Routing Problem with Private Capacitated Alternative Fuel Stations (GVRP-PCAFS). METS incorporates three key novelties that strengthen the coordination between global and local search processes. The effectiveness of METS has been validated through extensive experiments on both existing benchmark sets and a newly introduced large-scale benchmark set based on real-world logistics data. Compared to existing approaches, METS discovered new best-known solutions on 31 out of 40 benchmark instances, achieving substantial improvements in solution quality.

Several promising directions for future research can be identified. First, the proposed SCTS strategy, which generates diverse solutions by considering different constraints separately, combined with the fitness evaluation function for controlling diversity and feasibility, presents a new general idea of applying EAs to solve various VRP variants with complex constraints. Hence, we plan to explore this idea on other VRP variants beyond GVRP-PCAFS. Second, extending GVRP-PCAFS into a multi-objective optimization framework could address practical needs by balancing travel time with service quality and fleet utilization while ensuring customer satisfaction [37]. Third, applying METS to more dynamic and complex logistics scenarios, particularly extra-large benchmark instances [38], would enhance its effectiveness and scalability in real-world applications. Finally, given recent advances in using large language models (LLMs) for solving routing problems [39], [40], investigating the integration of METS with LLMs for parameter recommendation and operator design presents an interesting research direction.

REFERENCES

[1] S. Erdoğan and E. Miller-Hooks, "A green vehicle routing problem," *Transp. Res. E: Logist. Transp. Rev.*, vol. 48, no. 1, pp. 100–114, 2012.
[2] M. Asghari, S. M. J. M. Al-e *et al.*, "Green vehicle routing problem: A state-of-the-art review," *Int. J. Prod. Econ.*, vol. 231, p. 107899, 2021.
[3] Y.-H. Jia, Y. Mei, and M. Zhang, "Confidence-based ant colony optimization for capacitated electric vehicle routing problem with comparison of different encoding schemes," *IEEE Trans. Evol. Comput.*, vol. 26, no. 6, pp. 1394–1408, 2022.
[4] Z. Zheng, S. Liu, and Y.-S. Ong, "Hybrid memetic search for electric vehicle routing with time windows, simultaneous pickup-delivery, and partial recharges," *arXiv preprint arXiv:2410.19580*, 2024.
[5] B. Yıldız, E. Olcaytu, and A. Şen, "The urban recharging infrastructure design problem with stochastic demands and capacitated charging stations," *Transp. Res. B: Methodol.*, vol. 119, pp. 22–44, 2019.
[6] M. Bruglieri, S. Mancini, and O. Pisacane, "The green vehicle routing problem with capacitated alternative fuel stations," *Comput. Oper. Res.*, vol. 112, p. 104759, 2019.
[7] ——, "A more efficient cutting planes approach for the green vehicle routing problem with capacitated alternative fuel stations," *Optim. Lett.*, pp. 1–17, 2021.
[8] M. Bruglieri, D. Ferone, P. Festa, and O. Pisacane, "A grasp with penalty objective function for the green vehicle routing problem with private capacitated stations," *Comput. Oper. Res.*, vol. 143, p. 105770, 2022.
[9] P. He and J.-K. Hao, "Memetic search for the minmax multiple traveling salesman problem with single and multiple depots," *Eur. J. Oper. Res.*, vol. 307, no. 3, pp. 1055–1070, 2023.
[10] S. Liu, K. Tang, and X. Yao, "Memetic search for vehicle routing with simultaneous pickup-delivery and time windows," *Swarm Evol. Comput.*, vol. 66, p. 100927, 2021.
[11] R. Zhai, Y. Mei, T. Guo, and W. Du, "A collaborative drone-truck delivery system with memetic computing optimization," *IEEE Trans. Syst. Man Cybern.: Syst.*, 2024.
[12] G. Poonthalir and R. Nadarajan, "Green vehicle routing problem with queues," *Expert Syst. Appl.*, vol. 138, p. 112823, 2019.
[13] M. Keskin, G. Laporte, and B. Catay, "Electric vehicle routing problem with time-dependent waiting times at recharging stations," *Comput. Oper. Res.*, vol. 107, pp. 77–94, 2019.
[14] M. Keskin, B. Çatay, and G. Laporte, "A simulation-based heuristic for the electric vehicle routing problem with time windows and stochastic waiting times at recharging stations," *Comput. Oper. Res.*, vol. 125, p. 105060, 2021.
[15] X. Chen, Y.-S. Ong, M.-H. Lim, and K. C. Tan, "A multi-facet survey on memetic computation," *IEEE Trans. Evol. Comput.*, vol. 15, no. 5, pp. 591–607, 2011.
[16] Y.-S. Ong, M. H. Lim, and X. Chen, "Memetic computation—past, present & future [research frontier]," *IEEE Comput. Intell. Mag.*, vol. 5, no. 2, pp. 24–31, 2010.
[17] A. Lara, G. Sanchez, C. A. C. Coello, and O. Schutze, "Hcs: A new local search strategy for memetic multiobjective evolutionary algorithms," *IEEE Trans. Evol. Comput.*, vol. 14, no. 1, pp. 112–132, 2010.
[18] L. Ma, J. Li, Q. Lin, M. Gong, C. A. Coello Coello, and Z. Ming, "Cost-aware robust control of signed networks by using a memetic algorithm," *IEEE Trans. Cybern.*, vol. 50, no. 10, pp. 4430–4443, 2020.
[19] L. Beke, L. Uribe, A. Lara, C. A. C. Coello, M. Weiszer, E. K. Burke, and J. Chen, "Routing and scheduling in multigraphs with time constraints—a memetic approach for airport ground movement," *IEEE Trans. Evol. Comput.*, vol. 28, no. 2, pp. 474–488, 2023.
[20] Z. Lei and J.-K. Hao, "An effective memetic algorithm for the close-enough traveling salesman problem," *Appl. Soft Comput.*, vol. 153, 2024.
[21] T. Vidal, T. G. Crainic, M. Gendreau, N. Lahrichi, and W. Rei, "A hybrid genetic algorithm for multidepot and periodic vehicle routing problems," *Oper. Res.*, vol. 60, no. 3, pp. 611–624, 2012.
[22] S. Nucamendi-Guillén, D. Flores-Díaz, E. Olivares-Benitez, and A. Mendoza, "A memetic algorithm for the cumulative capacitated vehicle routing problem including priority indexes," *Appl. Sci.*, vol. 10, no. 11, 2020.
[23] J. Wang, W. Ren, Z. Zhang, H. Huang, and Y. Zhou, "A hybrid multiobjective memetic algorithm for multiobjective periodic vehicle routing problem with time windows," *IEEE Trans. Syst. Man Cybern.: Syst.*, vol. 50, no. 11, pp. 4732–4745, 2020.
[24] Z. Lei and J.-K. Hao, "A memetic algorithm for vehicle routing with simultaneous pickup and delivery and time windows," *IEEE Trans. Evol. Comput.*, 2024.
[25] K. Tang, S. Liu, P. Yang, and X. Yao, "Few-shots parallel algorithm portfolio construction via co-evolution," *IEEE Trans. Evol. Comput.*, vol. 25, no. 3, pp. 595–607, 2021.
[26] J. Xiao, J. Du, Z. Cao, X. Zhang, and Y. Niu, "A diversity-enhanced memetic algorithm for solving electric vehicle routing problems with time windows and mixed backhauls," *Appl. Soft Comput.*, vol. 134, 2023.

[27] C. Lavigne, D. Inghels, W. Dullaert, and R. Dewil, "A memetic algorithm for solving rich waste collection problems," *Eur. J. Oper. Res.*, vol. 308, no. 2, pp. 581–604, 2023.

[28] C. Prins, "A simple and effective evolutionary algorithm for the vehicle routing problem," *Comput. Oper. Res.*, vol. 31, no. 12, pp. 1985–2002, 2004.

[29] T. Vidal, T. G. Crainic, M. Gendreau, and C. Prins, "A unified solution framework for multi-attribute vehicle routing problems," *Eur. J. Oper. Res.*, vol. 234, no. 3, pp. 658–673, 2014.

[30] C. Prins, P. Lacomme, and C. Prodhon, "Order-first split-second methods for vehicle routing problems: A review," *Transp. Res. C: Emerg. Technol.*, vol. 40, pp. 179–200, 2014.

[31] A. Montoya, C. Guéret, J. E. Mendoza, and J. G. Villegas, "A multi-space sampling heuristic for the green vehicle routing problem," *Transp. Res. C: Emerg. Technol.*, vol. 70, pp. 113–128, 2016.

[32] S. Zhang, Y. Gajpal, and S. Appadoo, "A meta-heuristic for capacitated green vehicle routing problem," *Ann. Oper. Res.*, vol. 269, pp. 753–771, 2018.

[33] L. Wang and J. Lu, "A memetic algorithm with competition for the capacitated green vehicle routing problem," *IEEE/CAA J. Autom. Sin.*, vol. 6, no. 2, pp. 516–526, 2019.

[34] L. Davis, "Applying adaptive algorithms to epistatic domains," *Proc. Int. Jt. Conf. Artif. Intell.*, vol. 1, pp. 162–164, 1985.

[35] K. Helsgaun, "An effective implementation of the lin–kernighan traveling salesman heuristic," *Eur. J. Oper. Res.*, vol. 126, no. 1, pp. 106–130, 2000.

[36] M. López-Ibáñez, J. Dubois-Lacoste, L. Pérez Cáceres, M. Birattari, and T. Stützle, "The irace package: Iterated racing for automatic algorithm configuration," *Oper. Res. Perspect.*, vol. 3, pp. 43–58, 2016.

[37] Y. Xiang, X. Yang, H. Huang, and J. Wang, "Balancing constraints and objectives by considering problem types in constrained multiobjective optimization," *IEEE Trans. Cybern.*, vol. 53, no. 1, pp. 88–101, 2021.

[38] X. Ma, Z. Huang, X. Li, L. Wang, Y. Qi, and Z. Zhu, "Merged differential grouping for large-scale global optimization," *IEEE Trans. Evol. Comput.*, vol. 26, no. 6, pp. 1439–1451, 2022.

[39] S. Liu, C. Chen, X. Qu, K. Tang, and Y.-S. Ong, "Large language models as evolutionary optimizers," in *Proceedings of the 2024 IEEE Congress on Evolutionary Computation (CEC)*, Yokohama,Japan, 2024, pp. 1–8.

[40] X. Wu, S.-h. Wu, J. Wu, L. Feng, and K. C. Tan, "Evolutionary computation in the era of large language model: Survey and roadmap," *IEEE Trans. Evol. Comput.*, vol. 29, no. 2, pp. 534–554, 2025.